Achievable Performance of Bayesian Compressive Sensing Based Spectrum Sensing

Mehmet Başaran,[1] Serhat Erküçük,[2] and Hakan Ali Çırpan[1]
[1]Istanbul Technical University, Department of Electronics and Communications Engineering, Istanbul, Turkey
[2]Kadir Has University, Department of Electrical-Electronics Engineering, Istanbul, Turkey
E-mail: {mehmetbasaran, cirpanh}@itu.edu.tr, {serkucuk}@khas.edu.tr

***Abstract*—In wideband spectrum sensing, compressive sensing approaches have been used at the receiver side to decrease the sampling rate, if the wideband signal can be represented as sparse in a given domain. While most studies consider the reconstruction of primary user's signal accurately, it is indeed more important to analyze the presence or absence of the signal correctly. Furthermore, these studies do not consider the achievable lower bounds of reconstruction error and how well the selected method performs correspondingly. Motivated by these issues, we investigate in detail the primary user detection performance of Bayesian compressive sensing (BCS) approach in this paper. Accordingly, we (i) determine the BCS signal reconstruction performance in terms of mean-square error (MSE), compression ratio and signal-to-noise ratio (SNR), and compare it with the conventionally used basis pursuit approach, (ii) determine how well BCS performs compared with the Bayesian Cramer-Rao lower bound (BCRLB) of the signal reconstruction error, and (iii) assess the probability of detection performance of BCS for various SNR and compression ratio values. The results of this study are important for determining the achievable performance of BCS based spectrum sensing.**

Keywords—Cognitive radios, ultra wideband (UWB) systems, energy efficiency, Bayesian compressive sensing, spectrum sensing, probability of detection

I. Introduction

Energy efficiency is one of the main concerns of wireless communication systems. One major factor that causes energy loss in a wireless device is the high rate sampling at the transceiver side. While communicating with wideband signaling, which in turn can provide higher data rates, the receiver has to operate at high sampling rates in order to satisfy the Nyquist sampling theorem. This may result in energy loss and reduce the battery life of the wireless device. If the device can operate at a sampling rate lower than the Nyquist rate without losing any information, then the device will be energy-efficient in terms of sampling operation. This is possible through the *compressive sensing* (CS) theory introduced in [1] and [2]. According to the CS theory, under certain conditions it is sufficient to collect only a small number of signal observations (obtained at sub-Nyquist rate) and still be able to reconstruct the original signal if the signal admits a sparse representation in a given basis or domain [3]. This theory has found great interest also in the area of spectrum sensing, where the frequency-domain representation is assumed to be sparse for wideband spectrum sensing [4], [5]. Similarly, in ultra wideband (UWB) communications, the frequency band in the order of 500 MHz may be occupied by a few primary users in different frequency bands. These primary users must be detected before the wideband or UWB system can start communicating, where the primary users can be detected using energy detection in time-domain [6]. On the other hand, the detection of these systems in frequency-domain would yield a sparse structure as not all frequency bands of UWB systems are generally occupied.

Most of the wideband spectrum sensing studies that use the CS approach have focused on the reconstruction of primary user's signal accurately. However, it is more important to determine the presence or absence of the primary user's signal in spectrum sensing. Furthermore, these studies do not consider the achievable lower bounds of signal reconstruction error and how well the selected method performs correspondingly [4], [5]. In [7], the Bayesian compressive sensing (BCS) approach proposed in [8] was applied to spectrum sensing so as to compute signal parameter estimation recursively. It was claimed that the entire signal did not have to be reconstructed and only the detection of primary user is of interest. However, presented results included only the mean-square error (MSE) of signal reconstruction rather than the signal detection. In addition, a lower bound on the MSE was not provided to assess how well the BCS performed in spectrum sensing. In [9], the localization of the primary users was incorporated into the BCS based spectrum sensing framework of [7]. However, presented results did not include the effects of compression ratios and the signal-to-noise ratio (SNR) on the detection performance.

Motivated by applying the Bayesian framework in [8] to spectrum sensing and by determining the primary user detection performance limits, which were not addressed in [7] and [9], we study the primary user detection performance of BCS based spectrum sensing. Specifically, we (i) determine the BCS signal reconstruction performance in terms of MSE under different compression ratios and SNR values, and compare it with the conventionally used basis pursuit approach [10], (ii) determine how well BCS performs compared with the Bayesian Cramer-Rao lower bound (BCRLB) of the signal reconstruction error, and (iii) assess the probability of detection performance of BCS for various SNR and compression ratio values. The results of this study are important for determining the achievable performance of BCS based spectrum sensing.

The rest of paper is organized as follows. In Section II, primary user signal model and the BCS theory that can be applied for spectrum sensing are explained. In Section III, performance measures of BCS based spectrum sensing are provided. In Section IV, simulation results are presented for performance comparison. Concluding remarks are given in Section V.

II. Bayesian CS for Primary User Detection

In this section, initially the primary user signal model will be presented followed by the application of BCS to estimate the signal parameters. The received signal sampled below Nyquist rate can be represented as

$$\mathbf{r} = \mathbf{A}\big(\mathbf{w}_t + \mathbf{n}_t\big) = \mathbf{A}\mathbf{F}^{-1}\mathbf{w}_f + \mathbf{A}\mathbf{n}_t = \mathbf{\Phi}\mathbf{w}_f + \mathbf{n} \quad (1)$$

where $\mathbf{A}$ is the $N \times M$ random measurement matrix ($N < M$), $\mathbf{w}_t$ denotes the Nyquist rate sampled time domain signal, and $\mathbf{n}_t$ represents the additive white Gaussian noise. The operation $\mathbf{F}^{-1}$ represents the inverse Fourier transform matrix, $\mathbf{w}_f$ is the frequency domain response of the time domain signal, $\mathbf{\Phi} = \mathbf{A}\mathbf{F}^{-1}$ defines the transition from frequency domain signal samples to time domain compressed observations and $\mathbf{n}$ is zero-mean Gaussian noise with variance σ^2. Note that if $\mathbf{w}_f$ exhibits a sparse structure, CS can be applied to estimate M-sample $\mathbf{w}_f$ from N-sample observations $\mathbf{r}$.

In Bayesian CS [8], the goal is to estimate the unknown parameters $\mathbf{w}_f, \boldsymbol{\beta}$ and α, where $\boldsymbol{\beta}$ is an $M \times 1$ hyperparameter vector controlling the precision (i.e., inverse variance) of the samples of $\mathbf{w}_f$ and $\alpha = 1/\sigma^2$ is a hyperparameter scalar representing the noise precision. The full posterior distribution over all unknowns of interest can be written as

$$p(\mathbf{w}_f, \boldsymbol{\beta}, \alpha|\mathbf{r}) = \frac{p(\mathbf{r}|\mathbf{w}_f, \boldsymbol{\beta}, \alpha)p(\mathbf{w}_f, \boldsymbol{\beta}, \alpha)}{p(\mathbf{r})}. \quad (2)$$

Unfortunately, the probability of observation vector, $p(\mathbf{r})$, defined by the following equation

$$p(\mathbf{r}) = \int\int\int p(\mathbf{r}|\mathbf{w}_f, \boldsymbol{\beta}, \alpha)p(\mathbf{w}_f, \boldsymbol{\beta}, \alpha)\, d\mathbf{w}_f d\boldsymbol{\beta} d\alpha \quad (3)$$

cannot be computed analytically. Hence, the full posterior distribution can be rewritten as

$$p(\mathbf{w}_f, \boldsymbol{\beta}, \alpha|\mathbf{r}) = p(\mathbf{w}_f|\mathbf{r}, \boldsymbol{\beta}, \alpha)p(\boldsymbol{\beta}, \alpha|\mathbf{r}). \quad (4)$$

The noise component, $\mathbf{n}$, can be modeled as an independent zero-mean Gaussian process whose probability can be defined as

$$p(\mathbf{n}) = \prod_{i=1}^{N} \mathcal{N}(n_i|0, \sigma^2). \quad (5)$$

Under a noisy environment, the observation vector $\mathbf{r}$ consisting of N observations can be expressed as

$$\begin{aligned} p(\mathbf{r}|\mathbf{w}_f, \alpha) &= \prod_{i=1}^{N} \mathcal{N}(\mathbf{\Phi}\mathbf{w}_f, \sigma^2) \quad (6) \\ &= (2\pi\sigma^2)^{-N/2} \exp\left(-\frac{1}{2\sigma^2}||\mathbf{r} - \mathbf{\Phi}\mathbf{w}_f||_2^2\right) \end{aligned}$$

where $||\cdot||_p$ represents ℓ_p-norm. At this point, a Gaussian prior on $\mathbf{w}_f$ can be defined so as to compute each coefficient of $\mathbf{w}_f$ yielding less computational time and better estimation performance when compared to the ℓ_1-norm estimation. Contrary to ℓ_1-norm estimation [10], prior information is used in BCS based parameter estimation. Defining a Gaussian prior on $\mathbf{w}_f$, the weight of each coefficient of $\mathbf{w}_f$ will depend on the prior information and can be expressed as [8]

$$\begin{aligned} p(\mathbf{w}_f|\boldsymbol{\beta}) &= \prod_{i=1}^{M} \mathcal{N}(w_{f,i}|0, \beta_i^{-1}) \quad (7) \\ &= \prod_{i=1}^{M} (2\pi\beta_i^{-1})^{-1/2} \exp\left(-\frac{\beta_i w_{f,i}^2}{2}\right), \end{aligned}$$

where $\mathbf{w}_f = [w_{f,1}, w_{f,2}, \ldots, w_{f,M}]^T$.

The first term of full posterior distribution given in (4) can be expressed utilizing Bayes' rule as

$$p(\mathbf{w}_f|\mathbf{r}, \boldsymbol{\beta}, \alpha) = \frac{p(\mathbf{r}|\mathbf{w}_f, \alpha)p(\mathbf{w}_f|\boldsymbol{\beta})}{p(\mathbf{r}|\boldsymbol{\beta}, \alpha)}. \quad (8)$$

The posterior distribution given above is Gaussian distributed with mean $\boldsymbol{\mu}$ and variance $\mathbf{\Sigma}$, as in [8], where

$$\begin{aligned} \boldsymbol{\mu} &= \alpha\mathbf{\Sigma}\mathbf{\Phi}^T\mathbf{r} \\ \mathbf{\Sigma} &= \big(\mathrm{diag}(\boldsymbol{\beta}) + \alpha\mathbf{\Phi}^T\mathbf{\Phi}\big)^{-1}. \quad (9) \end{aligned}$$

The second term on the right-hand side of (4) also has to be calculated to obtain the unknown parameter distribution. This is possible through the type-II maximum likelihood procedure by using relevance vector machine (RVM) [11]. Considering the Bayes' theorem, it can be shown that the posterior distribution $p(\boldsymbol{\beta}, \alpha|\mathbf{r})$ is proportional to $p(\mathbf{r}|\boldsymbol{\beta}, \alpha)$ for appropriately selected hyperparameter values [8]. The marginal likelihood function then can be calculated as

$$p(\mathbf{r}|\boldsymbol{\beta}, \alpha) = \int_{-\infty}^{+\infty} p(\mathbf{r}|\mathbf{w}_f, \alpha)p(\mathbf{w}_f|\boldsymbol{\beta})d\mathbf{w}_f \quad (10)$$

where $p(\mathbf{r}|\mathbf{w}_f, \alpha)$ and $p(\mathbf{w}_f|\boldsymbol{\beta})$ were defined in (6) and (7), respectively.

In order to maximize the marginal likelihood function, log-marginal likelihood can be used for simplicity. The log-marginal likelihood function can be given as [12]

$$\begin{aligned} \log\, p(\mathbf{r}|\boldsymbol{\beta}, \alpha) &= \log \int_{-\infty}^{+\infty} p(\mathbf{r}|\mathbf{w}_f, \alpha)p(\mathbf{w}_f|\boldsymbol{\beta})d\mathbf{w}_f \quad (11) \\ &= \frac{N}{2}\log\,\alpha - \frac{1}{2}(\alpha\mathbf{r}^T\mathbf{r} - \boldsymbol{\mu}^T\mathbf{\Sigma}^{-1}\boldsymbol{\mu}) \\ &- \frac{1}{2}\log|\mathbf{\Sigma}| - \frac{N}{2}\log(2\pi) + \frac{1}{2}\sum_{i=1}^{M}\log\,\beta_i. \end{aligned}$$

After taking the derivative of log-marginal likelihood function with respect to $\boldsymbol{\beta}$ and α, and equating it to zero results in the following expressions

$$\begin{aligned} \beta_m^{new} &= \frac{1 - \beta_m\Sigma_{mm}}{\mu_m^2} \quad (12) \\ \alpha^{new} &= \frac{M - \sum_{m=1}^{M}(1 - \beta_m\Sigma_{mm})}{||\mathbf{r} - \mathbf{\Phi}\boldsymbol{\mu}||_2^2} \end{aligned}$$

where Σ_{mm} is the m-th diagonal element of the covariance matrix and μ_m is the m-th posterior mean value. By calculating the hyperparameters iteratively, $\mathbf{\Sigma}$ and $\boldsymbol{\mu}$ given in (9) can be obtained for a convergence criterion, and the unknown signal can be estimated as

$$\hat{\mathbf{w}}_f = \boldsymbol{\mu}. \quad (13)$$

III. PERFORMANCE MEASURES

In order to evaluate the performance of BCS based spectrum sensing, MSE, a lower bound on the MSE, probability of detection and convergence rate will be defined as performance measures in the following.

A. Mean-Square Error and Bayesian Cramer Rao Lower Bound (BCRLB)

Initially, the mean-square of the signal reconstruction error can be defined as

$$MSE = ||\mathbf{w}_f - \hat{\mathbf{w}}_f||_2^2. \quad (14)$$

The estimated signal, $\hat{\mathbf{w}}_f$, will be computed iteratively using (1), (9), (12) and (13) for BCS. For ℓ_1-norm[1], $\hat{\mathbf{w}}_f$ will be estimated as [10]

$$\hat{\mathbf{w}}_f = \text{arg min } ||\mathbf{w}_f||_1 \text{ subject to } ||\mathbf{\Phi}\mathbf{w}_f - \mathbf{r}||_2 \leq \epsilon \quad (15)$$

where ϵ is the noise power and can be represented as $\epsilon \geq ||\mathbf{n}||_2$.

By observing only the MSE performance, one cannot understand whether the performance of the estimator under special conditions is best achieved or not. Therefore, a lower bound on the estimation error should be considered. A lower bound on the BCS, Bayesian Cramer Rao lower bound (BCRLB), was defined in [13] as

$$E\left[||\mathbf{w}_f - \hat{\mathbf{w}}_f||_2^2\right] \geq K\left(N\gamma + \frac{1}{\sigma^2}\right)^{-1} \quad (16)$$

where K denotes the number of nonzero samples in the spectrum, N denotes the number of observations and γ is the SNR calculated as $\gamma = \frac{\mathbf{w}_f^T\mathbf{\Phi}^T\mathbf{\Phi}\mathbf{w}_f}{\sigma^2}$. BCRLB given in (16) will be assessed in the next section. If the estimation performance is very close to BCRLB, then it can be inferred that the proposed estimator performs well.

B. Probability of Detection

Not only parameter estimation, but also signal detection is important in primary user detection. Assuming that the M-sample long spectrum can be represented by L orthogonal bands, the probability of detection of the l^{th} band can be expressed as

$$P_{d,l} = \text{Pr}\left[\hat{\mathbf{w}}_{f,l}^T\hat{\mathbf{w}}_{f,l} \geq \lambda \,|\, l^{th} \text{ band occupied}\right] \quad (17)$$

where λ is the threshold value and $\hat{\mathbf{w}}_{f,l}$ represents the frequency domain samples estimated in the l^{th} band. This is illustrated in Fig. 1 for the $M\times 1$ vector $\hat{\mathbf{w}}_f = [\hat{\mathbf{w}}_{f,1}, \hat{\mathbf{w}}_{f,2}, \ldots, \hat{\mathbf{w}}_{f,32}]$, where only the 2^{nd} band is occupied with 16 nonzero samples. In the case of a few active orthogonal primary users, the spectrum will exhibit a sparse structure. The detection performance will be assessed in the next section.

[1]For the implementation of (15), the codes provided by Candes and Romberg publicly available at http://users.ece.gatech.edu/~justin/l1magic/ are used.

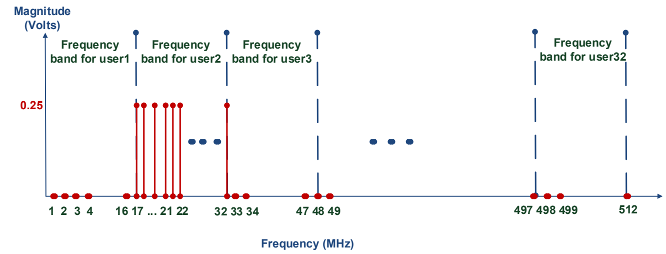

Fig. 1. Frequency domain sparse signal representation

C. Convergence Rate

While it was shown in [14] that BCS computation time is significantly shorter than ℓ_1-norm computation time under the same conditions, we will consider the BCS based estimator and explore the effects of compression ratio and SNR on its convergence in terms of number iterations. Accordingly, we will calculate the number of iterations to reach the convergence value of the inverse variance of the prior. For each nonzero spectrum coefficient, there is a converged value and it does not change much in the following iterations. In order to measure the required number of iterations, a stopping criterion can be given by considering the difference of the updated prior values with the previous values. The difference value, δ, can be defined as [12]

$$\delta = \sum_{i=1}^{M} |\beta_i^{n+1} - \beta_i^n| \quad (18)$$

where β_i^{n+1} and β_i^n represent inverse variance of the prior belonging to i^{th} hyperparameter at the $(n+1)^{th}$ and n^{th} iterations, respectively. When the difference value is smaller than a threshold value, δ_{thresh}, (i.e., $\delta < \delta_{thresh}$), iterations will stop. During the estimation process, $\boldsymbol{\beta}$ values corresponding to zero coefficients are pruned as the strength of the prior tends to go to infinity. Accordingly, it can be said that the variance of the prior goes to zero, where the coefficients of the spectrum are zero.

IV. SIMULATION RESULTS

In this section, primary user detection performance of BCS will be evaluated in terms of signal reconstruction error, probability of detection, and convergence rate. For the signal reconstruction error, the MSE performance as given in (14) will be compared to the BCRLB as given in (16), and to the performance of ℓ_1-norm as given in (15). For the probability of detection performance, energy values in each frequency band are compared with threshold values as in (17) for various SNR values and compression ratios. Throughout the simulations, it is assumed that the frequency domain signal representation consists of $M = 512$ samples, where there are possibly 32 orthogonal frequency division multiplexing (OFDM) signals in each 16-sample orthogonal bands. The sparsity ratio, which is defined as the ratio of the number of nonzero components K to the length of the spectrum M is selected as $16/512 = 1/32$ (i.e., one frequency band is occupied at a time). Compression ratios (i.e., N/M) are selected as $\{0.25, 0.375, 0.5, 0.75, 0.875\}$ and the energy of the frequency domain signal is normalized to unity.

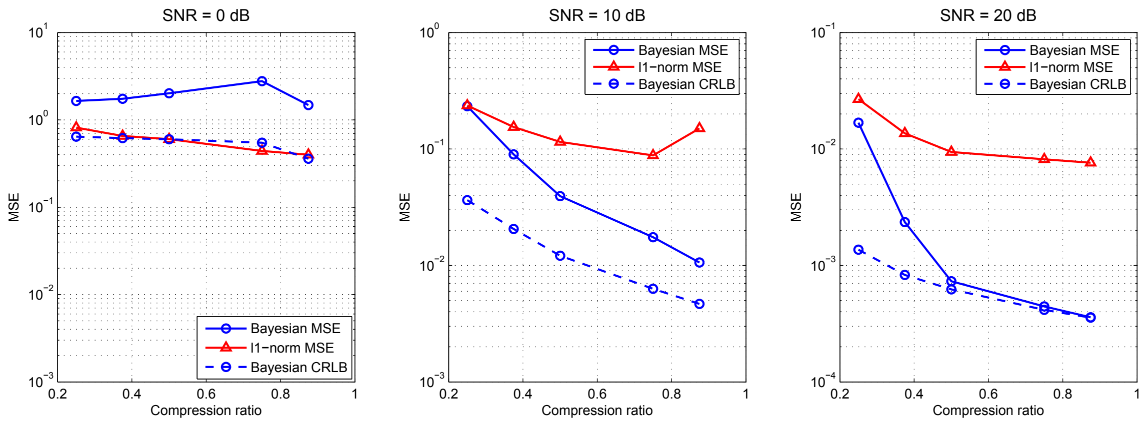

Fig. 2. Reconstruction error vs. compression ratio

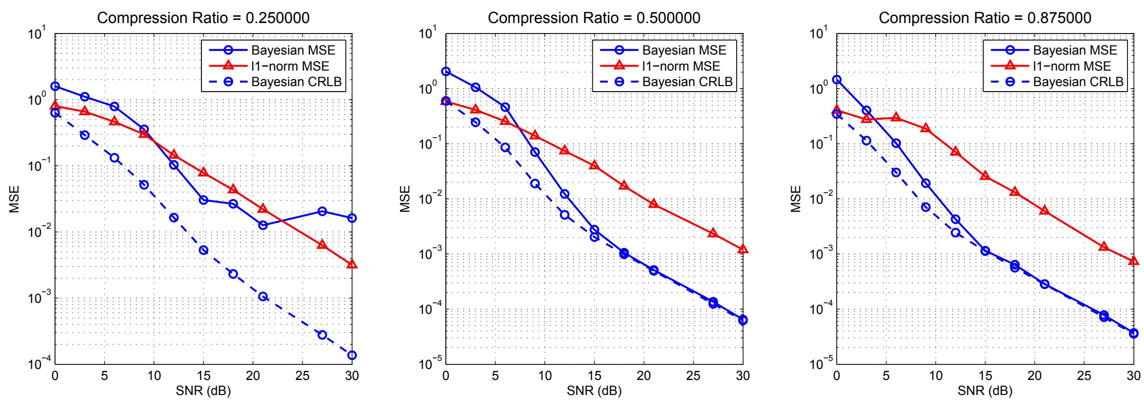

Fig. 3. Reconstruction error vs. SNR

In Fig. 2, reconstruction error performances of BCS and ℓ_1-norm based approach are plotted and compared with the BCRLB for various compression ratios at SNR=$\{0, 10, 20\}$dB. It can be observed that BCS performs inferior to the ℓ_1-norm approach in the low SNR region, however, it significantly outperforms ℓ_1-norm in medium- and high-SNR regions. Similar observations were made in [14] for BCS based channel estimation, where the inferior performance was explained with the uncertainty in the parameter estimation. Furthermore, it can be observed that the BCRLB is approached at high SNR values (e.g., SNR = 20dB) and compression ratios (e.g., $N/M \geq 0.5$).

Fig. 3 presents the reconstruction error performances of BCS and ℓ_1-norm for various SNR values at compression ratios $N/M = \{0.25, 0.5, 0.875\}$. It can be inferred that sensing performances improve with increasing compression ratios as expected, and approach the BCRLB. It is also important to note that the selection of 50% compression ratio is adequate as BCS achieves similar performance to that of BCRLB in medium- and high-SNR regions, and the sensing performances do not improve much when the compression ratio further increases to 87.5%. Hence, 50% sampling rate can be used to sense the primary user spectrum yielding energy efficiency.

In Figs. 4 and 5, probability of detection performances are plotted for various compression ratios and SNR values. It can be observed that probability of detection improves with increasing SNR and compression ratios as expected. When SNR = 20dB, probability of detection is greater than 90% for the selected threshold values. On the other hand, when the compression ratio is 0.875, probability of detection is greater than 90% for threshold values $\lambda = \{0.5, 0.75\}$. While lower threshold values provide better probability of detection, fixing the threshold to a low value may increase the *probability of false alarm*. This trade-off is not well investigated in the CS based spectrum sensing literature, and is of interest for our future study.

Finally, the convergence rate is assessed for BCS in terms of sufficient number of iterations required to converge for various SNR and compression ratio values. In our simulation scenario, we assume that there are 16 nonzero coefficients located in the 17–32 MHz band interval. In order to find the sufficient number of iterations, the threshold value is selected as $\delta_{thresh} = 0.01$ and compared with (18). The measurements are averaged over 100 trials. Table I shows the sufficient number of iterations under specific SNR and compression ratio values. It can be seen from Table I that the iteration number decreases with increasing SNR for a fixed compression ratio, as expected. On the other hand, the iteration number decreases with increasing compression ratio only for medium- and high-SNR regions. When SNR = 0dB, the iteration number increases with increasing compression ratio due to unreliable communications. This observation is consistent with the results of Fig. 2 (cf. the leftmost plot). In summary, looking from convergence rate aspect, the prior strength converges more quickly with increasing SNR and compression ratio.

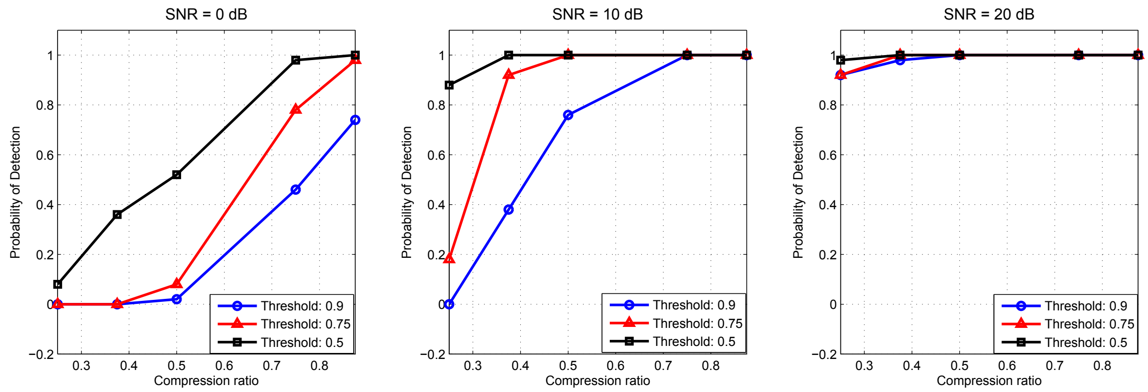

Fig. 4. Probability of detection vs. compression ratio

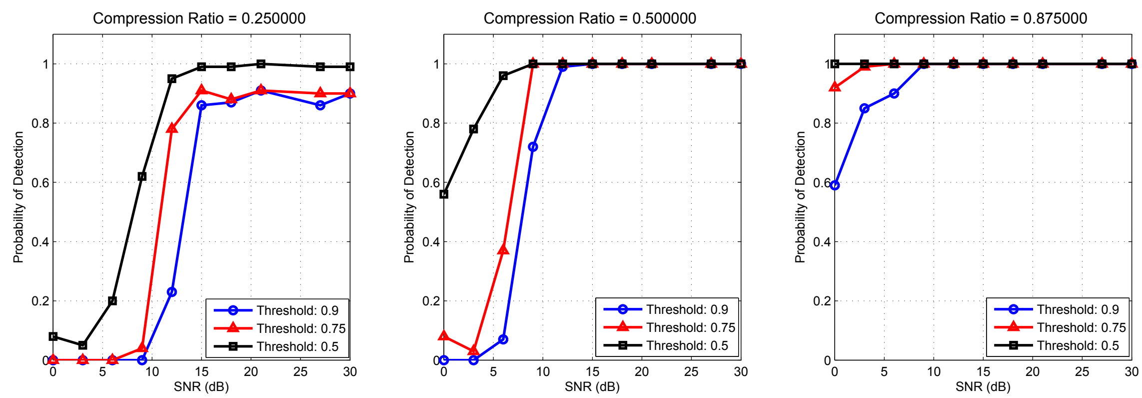

Fig. 5. Probability of detection vs. SNR

TABLE I. NUMBER OF ITERATIONS FOR CONVERGENCE

Compression Ratio	**SNR 0 dB**	**SNR 10 dB**	**SNR 20 dB**
0.25	25	22	6
0.50	42	16	5
0.875	50	9	4

V. CONCLUSION

In this paper, the implementation of BCS was considered for wideband spectrum sensing. Primary user detection performance was assessed in terms of signal reconstruction error and probability of detection, and compared with the ℓ_1-norm approach and the BCRLB. Simulation results show that BCS outperforms ℓ_1-norm approach in medium- and high-SNR regions with higher compression ratios. Furthermore, it is observed that the BCRLB can be attained at the high-SNR region with appropriate selection of compression ratio values. For successful detection of primary users, parameters investigated in this study should be carefully considered for practical implementation of BCS based spectrum sensing.

ACKNOWLEDGMENT

These initial research results have been obtained in preparation of a project proposal for TÜBİTAK (The Scientific and Technological Research Council of Turkey) under project ID 91577 and project no. 114E298.

REFERENCES

[1] E.J. Candes, J. Romberg, and T. Tao, "Robust uncertainty principles: exact signal reconstruction from highly incomplete frequency information," *IEEE Trans. Info. Theory*, vol. 52, pp. 489–509, 2006.

[2] D. Donoho, "Compressed sensing," *IEEE Trans. Info. Theory*, vol. 52, pp. 1289–1306, 2006.

[3] W.U. Bajwa, G. Leus, A. Scaglione, M. Stojanovic, and Z. Tian, "Guest editorial: special issue on compressive sensing in communications," *Physical Commun.*, vol. 5, pp. 61–63, 2012.

[4] Z. Tian and G. Giannakis, "Compressed sensing for wideband cognitive radios," in *ICASSP 2007*, pp. 1357–1360.

[5] Y. Gang, B. Zheng, and J. Chen, "Secure enhanced compressed wideband spectrum sensing," in *WCSP 2012*, pp. 1–5.

[6] B. Yilmaz and S. Erkucuk, "Detection of interdependent primary systems using wideband cognitive radios," *Intl. J. Electron. Commun. (AEUE)*, vol. 67, pp. 926–936, Nov. 2013.

[7] S. Hong, "Direct spectrum sensing from compressed measurements," in *MILCOM 2010*, pp. 1187–1192.

[8] S. Ji, Y. Xue, and L. Carin, "Bayesian compressive sensing," *IEEE Trans. Signal Process.*, vol. 56, no. 6, pp. 2346–2356, 2008.

[9] X. Li, S. Hong, Z. Han, and Z. Wu, "Bayesian compressed sensing based dynamic joint spectrum sensing and primary user localization for dynamic spectrum access," in *GLOBECOM 2011*, pp. 1–5.

[10] E.J. Candes and M.B. Wakin, "An introduction to compressive sampling," *IEEE Signal Processing Magazine*, vol. 25, no. 2, pp. 21–30, 2008.

[11] M.E. Tipping, "Sparse bayesian learning and the relevance vector machine," *Journal of Machine Learning Research*, vol. 1, pp. 211–244, 2001.

[12] T. Fletcher, "Relevance vector machines explained," (Tutorial Paper), http://www.tristanfletcher.co.uk/RVM Explained.pdf, Oct. 2010.

[13] H. Zayyani, M. Babaie-Zadeh, and C. Jutten, "Compressed sensing block map-lms adaptive filter for sparse channel estimation and a bayesian cramer-rao bound," in *MLSP 2009*, pp. 1–6.

[14] M. Ozgor, S. Erkucuk, and H.A. Cirpan, "Bayesian compressive sensing for ultra-wideband channel models," in *TSP 2012*, pp. 320–324.